Assembly and alignment of the 4-metre multi-object spectroscopic telescope wide field corrector

Mark H. Cunningham[ID],[a,][*] Peter Doel,[a] David Brooks,[a] Joar Brynnel,[b] Roelof S. de Jong[ID],[b] Steffen Frey[ID],[b] Michael Schroeck,[b] Miklos Gaebler,[b] Daniel Sablowski[ID],[b] and Sam C. Barden[ID][c]

[a]University College London, London, United Kingdom
[b]Leibniz Institute for Astrophysics Potsdam, Potsdam, Germany
[c]Canada France Hawaii Telescope, Kamuela, Hawaii, United States

Abstract. The 4-metre multi-object spectroscopic telescope (4MOST) is a fiber-fed multi-object spectrograph for the VISTA telescope at the European Southern Observatory (ESO) Paranal Observatory in Chile. The goal of the 4MOST project is to create a general purpose and highly efficient spectroscopic survey facility for astronomers in the 4MOST consortium and the ESO community. The instrument itself will record 2436 simultaneous spectra over a ~4.2 square deg field of view and consists of an optical wide-field corrector (WFC), a fiber positioner system based on a tilting spine design, and three spectrographs giving both high and low spectral dispersion. The WFC comprises of six lenses grouped into four elements, two of which are cemented doublets that act as an atmospheric dispersion corrector. The first lens element is 0.9 m in diameter while the diameter of the other elements is 0.65 m. For the instrument to meet its science goals, each lens was aligned to be well within ~100 μm—a major challenge. This was achieved using contact metrology methods supplemented by pencil beam laser probes. In particular, an off-axis laser beam system has been implemented to test the optics' alignment before and after shipment. This work details the alignment and assembly methods and presents the latest results on the achieved lens positioning and projected performance of the WFC. © *2023 Society of Photo-Optical Instrumentation Engineers (SPIE)* [DOI: 10.1117/1.JATIS.9.1.015002]

1 Introduction

Spectroscopy will always be fundamental when it comes to ground-based astronomy, yielding unique astrophysical insights such as the chemical composition and nature of stellar populations in nearby galaxies along with accurate red-shifts and the ionizing radiation field of extra-galactic sources.[1] As technology and engineering continue to make great leaps, it is of no surprise that in the last decade there have been incredible strides in optical and infrared (IR) imaging, with follow-up spectroscopy and telescope updates and reconfiguration becoming the status-quo. This has lead to large investment into multi-object spectroscopic facilities. As the name suggests, multi-object spectroscopy (MOS) is used to obtain simultaneous spectra of many objects. MOS uses multiple slits, mirrors, or optical fibers at the focal plane, to separate the light of many astronomical objects within a single field of view for spectral analysis. They allow multiple individually resolved spectra to be obtained per exposure and as such are ideal instruments for efficient large-scale, wide-field spectroscopic surveys. One such instrument is the 4-metre multi-object spectroscopic telescope (4MOST).

4MOST is a new spectroscopic survey facility that will provide the highest target multiplex on the largest field-of-view (FoV) in the southern hemisphere. The instrument is to be installed

---

*Address all correspondence to Mark H. Cunningham, mark.cunningham.20@ucl.ac.uk

on the 4.1-m visible and IR survey telescope for astronomy (VISTA) of the European Southern Observatory (ESO), located at the Paranal Observatory in Chile. The instrument will complement and enhance the results of many large-area sky surveys, such as four space-based observatories of prime European interest: Gaia, eROSITA, Euclid, and PLATO, and many ground-based facilities, such as very large telescope (VLT), VISTA, DECam, Vera C. Rubin Observatory, and square kilometer array (SKA). The science programme of the 4MOST consortium is structured into ten surveys, each pursuing different science cases; five dedicated to galactic archaeology and five dedicated to extra-galactic objects, including one of the most complete spectroscopic surveys of active galactic nuclei ever undertaken. In addition, fifteen science program led by European Space Agency (ESA) community scientists will be executed during the first 5-year survey of 4MOST.[2]

1.1 Instrument Overview

4MOST will provide spectral resolution high enough to detect chemical and kinematic substructure in the stellar halo, bulge, and disks of the Milky Way, and enough wavelength coverage to secure receding velocities of extra-galactic objects over a large range in red-shift.[3] Its wide field corrector (WFC) creates a 4.2 square deg FoV on the focal surface, where 2436 optical fibers positioned by the Australian–ESO Positioner (AESOP)[4] lead the light to two resolution $R \sim 5000$ spectrographs and one $R \sim 20,000$ spectrograph. This will yield more than 20 million spectra at resolution $R \sim 5000$ ($\lambda = 370 - 950$ nm) and more than 2 million spectra at $R \sim 20,000$ ($\lambda = 392.6 - 435.5, 516\text{-}573, 610\text{-}679$ nm) over the duration of the surveys conducted by 4MOST.[2]

A metrology system supports the accurate positioning of the fibers in the focal surface, while a calibration system provides the illumination from the M2 support spiders for wavelength and flat-field calibration. Figures 1 and 2 show in detail the 4MOST instrument including the WFC.

In order for the project to carry out its ambitious science goals the optical performance of the instrument is critical. This places tight tolerances on the manufacture and alignment of the WFC optics (Table 1). In particular, precise micrometre scale alignment is required which is a major challenge in any astronomical instrument assembly. In this paper, we outline the metrology methods used to precisely measure the elements of the WFC and present the results of the alignment and assembly of the WFC lenses along with the processes used.
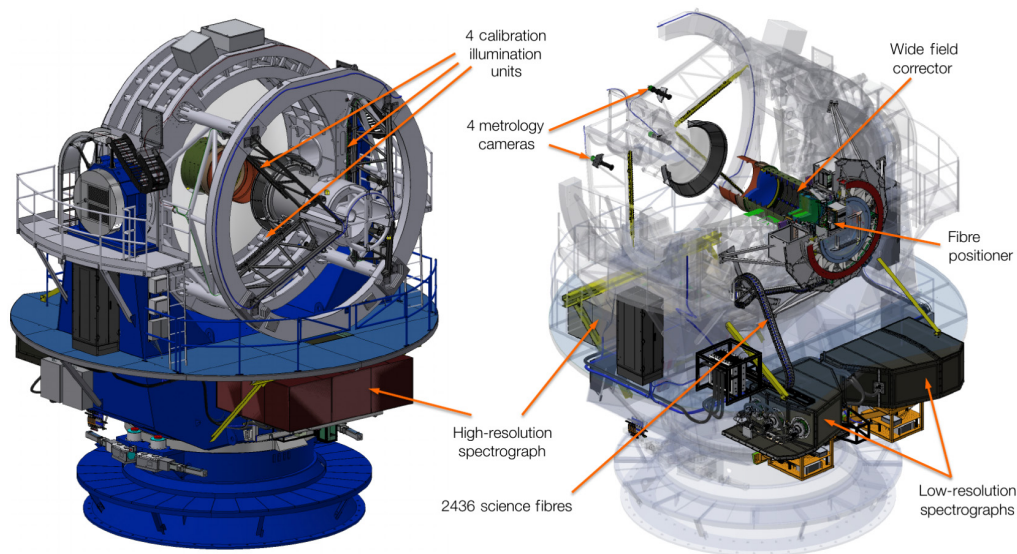

Fig. 1 Physical layout of the 4MOST elements on the VISTA telescope with the main components labeled. (Image credit: 4MOST consortium).
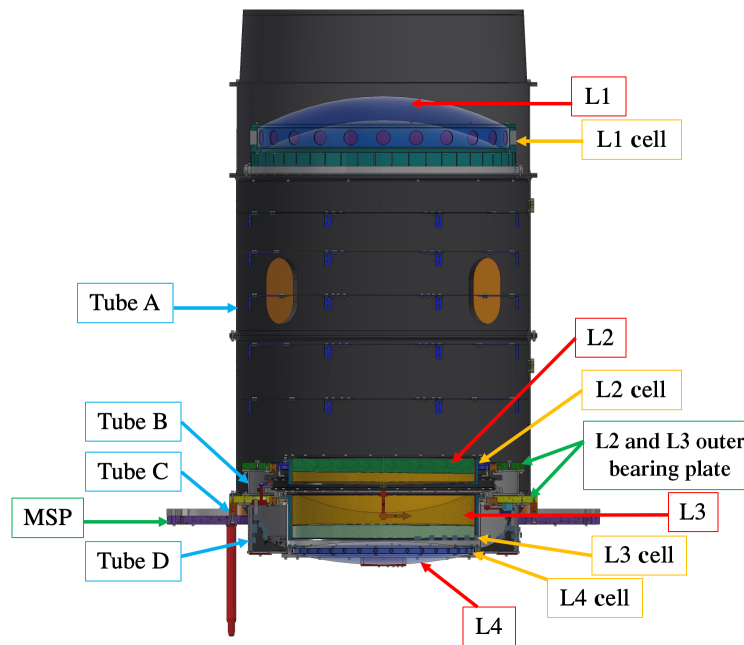
Fig. 2 Labeled drawing of WFC with the main components.

Table 1 Lens element position tolerances. Axial tolerance is ±200 μm for each element.

Element	Decenter ($\pm\mu$m)	Tilt ($\pm\mu$rad)	Tilt run out across diameter ($\pm\mu$m)
L1	200	873	785
L2	1000	1454	945
L3	100	145	95
L4	200	218	142

1.2 Optical Design

The WFC is a key optical component for the 4MOST facility in that it performs the critical image correction to the VISTA telescope optics in order to deliver the requisite field of view, image quality and plate scale; all of which are crucial for the science cases.[5] The WFC consists of six lenses grouped in four parts, two of which act as doublets that make up the atmospheric dispersion corrector (ADC) unit. The positions of the lenses are shown in Fig. 3, labeled L1, L2, L3, and L4. The lenses were manufactured at KiwiStar Optics, New Zealand and anti-reflection coated by Coherent in the United States, before being shipped to University College London (UCL) for integration and assembly. Further discussion and details of the optical specifications can be found in Azais et al. 2016.[5]

Each lens is mounted in a lens cell which acts as an interface to the main barrel assembly. The ADC lens cells are mounted on interfaces (bearing plates) that can rotate as part of the ADC action. The main structural plate (MSP) connects via a spacer to the telescope Cassegrain rotator.

1.3 General Assembly

The general assembly for the WFC is described in the flow diagram in Fig. 4. It has been broken down into three main stages. Preassembly describes the initial work done to allow the "dry" assembly and the final assembly to be carried out. The "dry" assembly describes the alignment and procedure that was followed without the lenses installed, this was carried out to give an indication of how the WFC would come together during the final assembly and how different
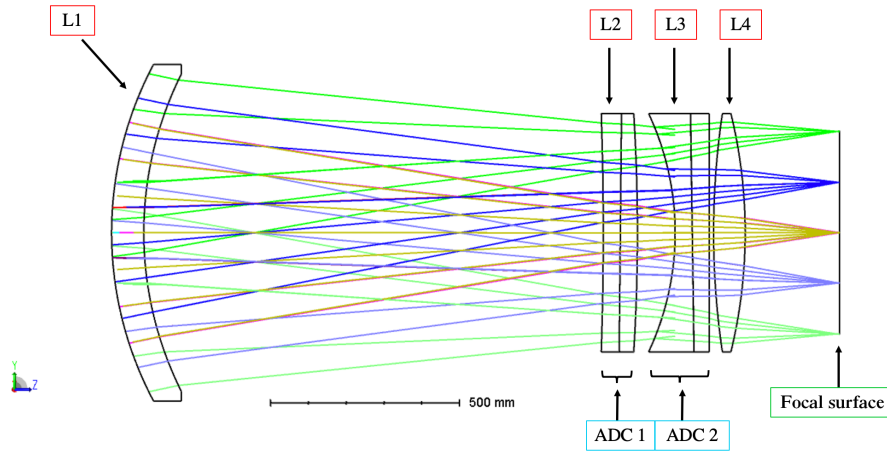
Fig. 3 Optical layout of the WFC lenses, showing different focus positions for different field angles. This shows that all the lenses contribute in correcting the incoming light to produce high quality images across the focal plane.
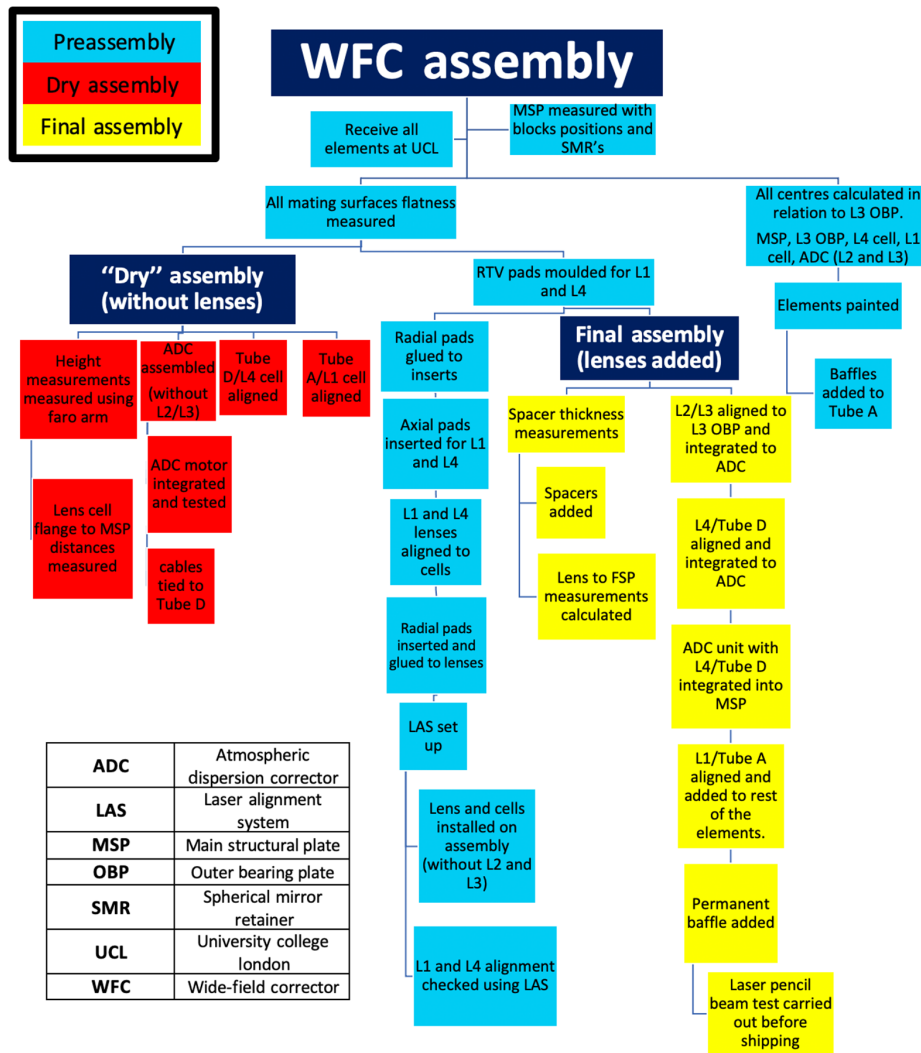

Fig. 4 Flow diagram showing the general process of alignment and assembly for the WFC at UCL. The key on the right shows the different stages of assembly. This process chart shows the general procedure that was followed during the building and assembly of the WFC.

surfaces mated with each other. The dry assembly also gave an opportunity to measure the position of the various surfaces which are then used in the derivation of the spacer thicknesses (metal shims that need to be installed at specified locations on the WFC to maintain the correct relative axial position for the optics). During this measurement phase, all lens cells were aligned to a chosen axis and locked in location using retractable pins. The final assembly describes the last stage of assembling the WFC, after all individual measurements have been taken and lenses were potted in their cells. During this stage, all elements are integrated and aligned together as described in 4.

2 Alignment Strategy

The alignment technique adopted was to use precision metrology of the components to position them to the required accuracy. The metrology methods used were a Faro gage arm, and digital dial gauges coupled with a precision rotary table (see Fig. 5 for image of dial gauges and Table 4 for instrument accuracy's). A check on the position of the lenses was made using a pencil beam laser alignment system (LAS). Dial gauges were used for surface flatness measurements as well as for center runout measurements. The Faro gage arm was used for height measurements and to map out surfaces from which heights could be derived. A micrometer and vernier calipers were also used for sections of the assembly including the height measurements of the tube A barrel and a laser displacement sensor (LDS) was used to measure the heights of the room temperature vulcanised (RTV) rubber axial pads that supported the lenses when placed into their cells. A laser and camera system was also used to optically test the alignment of L1 and L4, details of which can be found in Sec. 6. Individual lens position tolerances for the WFC are detailed in Table 1.

Generally throughout the measurements, a 1-24 numbering system was used to mark angular position on each component, with each position corresponding to the evenly spaced bolt holes on the ADC bearing plates. The first position No. 1 started at +X and the rotary table was turned anticlockwise until No. 24. These positions were marked on the other elements so that the same numbering system remained consistent. In positions where the ADC coordinate/numbering system was not used, (mainly for the MSP) a 1-36 numbering system was used that again corresponded to evenly spaced holes on the MSP with No. 1 stating at +X and the rotary table turning clockwise until No. 36 (No. 1 is defined as being along the +X axis throughout).

Fig. 5 Image showing dial gauge measurements being taken of the both the L1 lens and L1 cell.

First, a reference position to align the components to in the system was established. This was chosen to be the center position of the L3 outer bearing plate (OBP). The L3 OBP was chosen as this was a very circular surface and was in position during the majority of measurements when all the lens and barrel components were being measured. The measurement of the L3 OBP center was performed using dial gauges on the outer diameter every time a new construction or alignment was carried out and the position of the WFC components referenced back to this position. During each remeasurement of the L3 OBP center the plate was aligned such that its center was within 10 μm of the rotary table axis.

3 Lens-Cell and Barrel Alignment

Each lens of the WFC had a requisite tolerance to which they were to be mounted into their respective lens cells. A full description of the optical prescription data can be found in Azais et al.[5] The lenses as shown in Fig. 3, describe the optical lens layout with L1 being the largest lens at 0.9m in diameter and with the only aspheric surface, while the rest of the lenses (L2, L3, and L4) being 0.65 m in diameter. UCL was responsible for the alignment and mounting of the L1 and L4 lenses into their respective cells, while Kiwistar Optics were responsible for the mounting of the L2 and L3 lenses into their cells. UCL was then tasked with reviewing the manufacturing tolerances of L2 and L3 as well as integrating all of these lenses with the ADC unit, and full assembly.

Accurate measurements of the elements interfaces and mating surfaces such as the cell flange surfaces were first produced. These included the L1 cell flange which connected to Tube A, the L3 OBP plate surface which mated with the bottom of Tube A and finally the MSP. This measurement (of the flange positions) when combined with the lens crown to cell base measurements allowed a spacer thickness to be determined that would put the lens in the correct position relative to the focal plane. All measurements were within 100 μm of the nominal positions except for the L3 inner bearing plate flange to base of tube C which had a deviation of ∼300 μm from the nominal position (this was a manufacturing issue and had already been accounted for). These differences were adjusted using machinable spacers and were added to the final assembly to ensure the distance from each lens to the MSP/focal surface plane (FSP) was consistent with the optical design.

3.1 Alignment of L2 and L3

L2 and L3 form the ADC unit and sit very close together. As L2 and L3 had to be integrated into the ADC unit, the center of the L2 and L3 inner bearings had to be established as this would become the rotary axis of the lenses. To do this, the L3 inner bearing plate inner diameter was measured in four positions each rotated by 90 deg to understand how the center changed as the bearing is rotated. From this, the center was calculated by finding an average of the four positions. The same process was carried out for L2. Both the L2 and L3 inner bearing plates center were aligned to each other to be within ∼20 μm and aligned to the L3 OBP to within ∼40 μm.

Once the inner bearing centers were confirmed, the L2 and L3 lens surface and centers were measured (Figs. 6 and 7). The L2 lens top surface was measured using the dial gauges and gave a run out of ∼500 μm. A wedge was put into both L2 and L3 by Kiwistar Optics which was part of the manufacturing specification and was within the manufacturing tolerances. The initial measurements of L2 showed that it had ∼450 μm of run out due to the wedge on the surface of L2, along with an additional 50 μm of tilt relative to the cell flange. The L2 cell flange run out was then minimised and the top and bottom surfaces remeasured. The bottom surface was found to be tilted, giving a run out of ∼50 μm (which happened to be in the same direction as the wedge). In the final set up, there was an additional ∼40 μm of run out which is likely caused by the roughness of the mating surface. The L3 lens top surface was measured in the same way using the dial gauges and gave a total run out of 48 μm. The centers of the L2 and L3 lenses in the ADC unit were found in the same way as the inner bearing centers, by rotating the bearing axis by 90 deg (this time using the ADC motors that were tested at UCL) in four positions and finding an average.
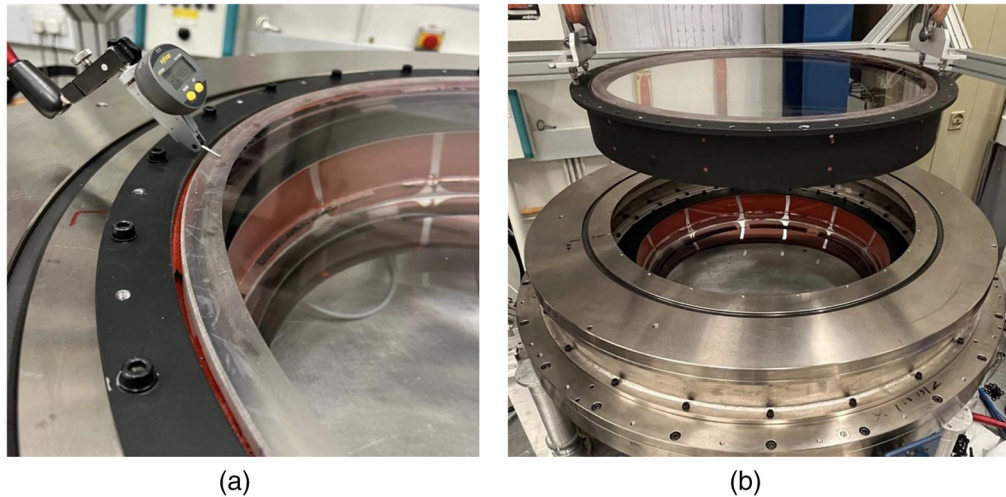
Fig. 6 (a) Image showing the L2 lens flat surface being measured by a dial gauge while in the ADC unit. (b) Showing L2 lens and cell being lowered into the ADC unit. In this image, the L3 lens is also visible.
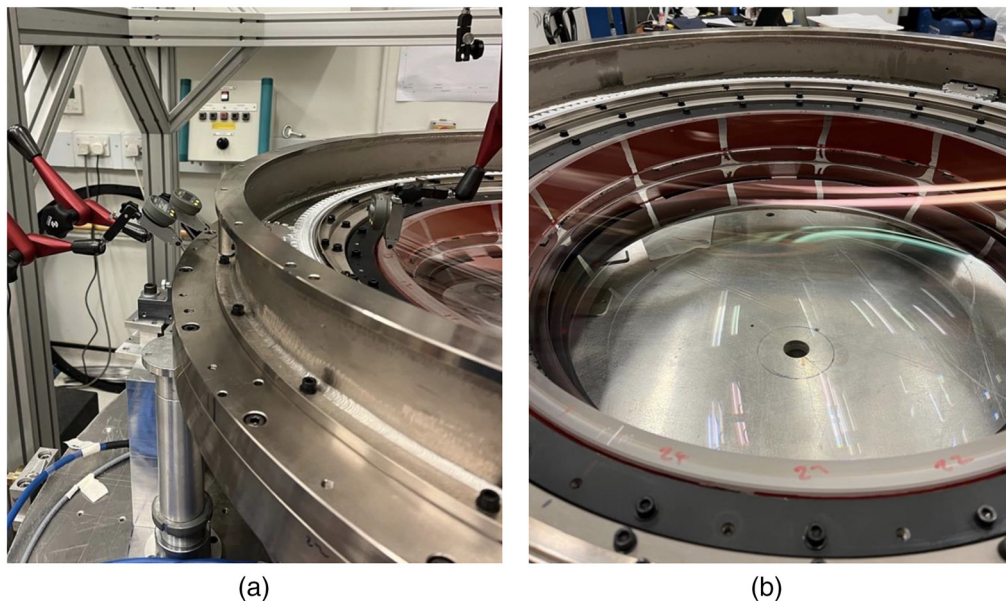

Fig. 7 (a) Image showing the L3 OBP and L3 lens being measured with dial gauges while supported on the rotary table using jacks. (b) Image showing a closeup of the L3 lens top surface in the ADC unit after measurements have been taken.

4 Lens to Cell Alignment

4.1 RTV Pads

Lenses were mounted to their cells using pads made from RTV560 silicone rubber. RTV rubbers are known to have a much higher coefficient of thermal expansion value (CTE) and so the high CTE of the RTV chosen can compensate for the difference in the CTEs between the lens and the cell.[6] There are two sets of pads, axial and radial pads in used during the potting of the lenses and the same procedure used to make the RTV pads in this work has been well documented in previous work,[7,8] (Fig. 8). Both the thicknesses of the axial and radial pads used to pot the lenses (L1 and L4) in this work are critical in the assembly of the WFC and finite element analysis (FEA)
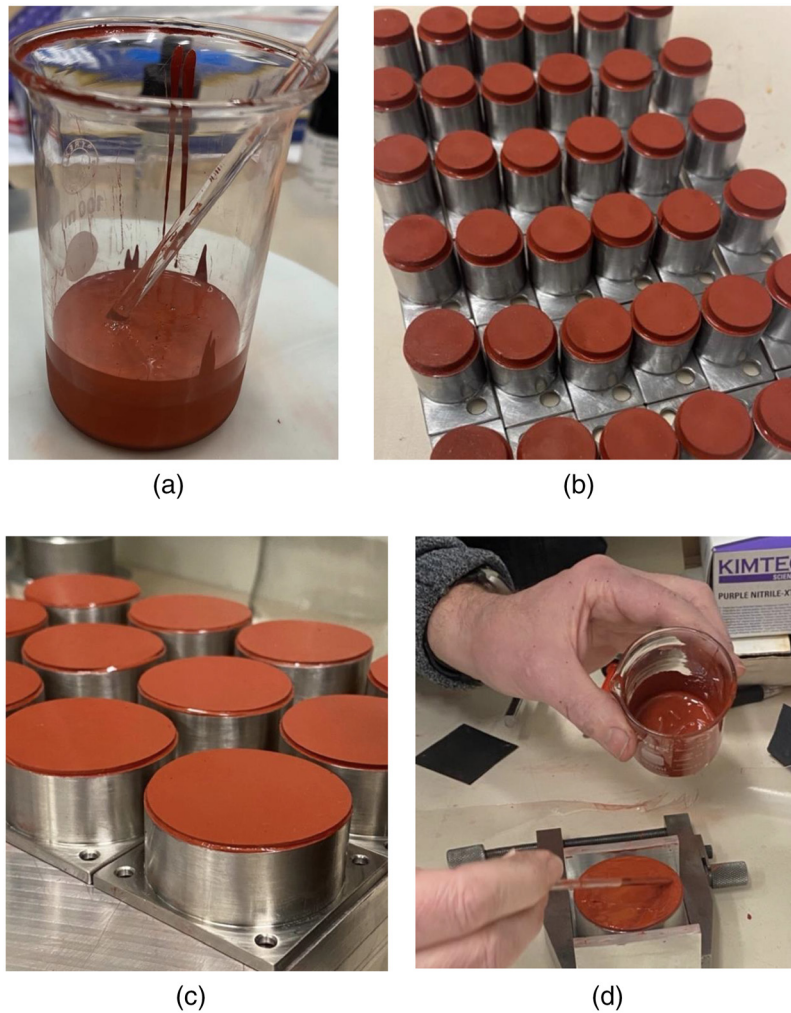
Fig. 8 (a) Image showing the RTV silicone rubber mixture before it would be placed into it moulds and left to cure for 24 hrs. (b) and (c) The L1 and L4 cell radial pads, respectively, that have been glued to the radial inserts for L1 and L4. (d) The inserts being given another coat of the silicone rubber mixture before being glued to the lens.

analysis was carried out prior to this work to determine the thickness and size of the RTV pads. The thickness of the pads were designed to make the lens-cell assembly essentially athermal to reduce induced stresses. A similar process of that tried and tested in the literature[6] was used for the potting of the L1 and L4 lenses at UCL. The process of making the RTV involved mixing the RTV560 base compound and the curing agent together as shown in Fig. 8, which was then degassed in a vacuum until the bubbling of the mixture stopped. The mixture was then placed into a mould (to ensure that all the pads were of uniform thickness, which was subsequently tested) where it was then left for 24 hrs to cure at room temperature. Once cured, it was released from the mould and cut into the correct size to be glued onto the lens cell inserts. Each lens was cleaned using isopropyl alcohol (Propan-2) before adding Momentive SS4004P as a primer to help with adhesion. The glue used for this process was RTV560 itself. The addition of primers such as Momentive SS4004P to the metal and glass allows the RTV to cure to these materials and creates a strong bond. The radial pads were then inserted through the cell and glued to the lens. This procedure was carried out for both the radial and axial pads for L1 and L4. Axial pads can be seen in Fig. 9(b).

After the initial lens cell flatness and surface measurements of the WFC elements were taken, the lenses were installed into their cells using the RTV pads as an interface between lens and cells. The axial pads are glued with a thin layer of RTV into the cells. The action of the axial pads is to support the lens evenly and take up any unevenness in the cell support surface. It is
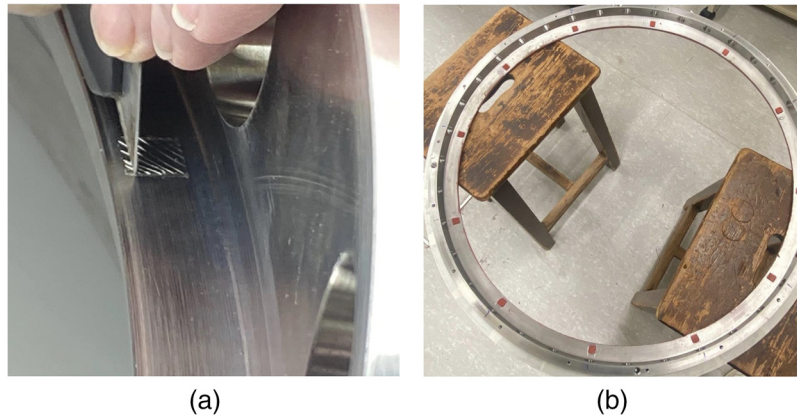
(a)   (b)

Fig. 9 (a) Image showing the process of scoring the surface of a cell where an RTV will be placed. The scratching of the cell aids in the RTV pad sticking to the cell along with the use of a primer. (b) Image showing the L4 cell with its 12 axial RTV pads (red squares) in place on the L4 angled surface, where the L4 lens will rest.

necessary for the axial pads to compress to comply for any pad height irregularities and lens but must also be stiff enough to hold the lens in place as the telescope moves away from its zenith position. The axial pads were installed such that their surfaces are on the same plane and parallel with the cell flange. During installation of the axial pads their surface position and height was verified using the LDS, and were found to be within 10 μm of the same plane (Fig. 10). The size of the RTV pads were chosen to achieve a uniform support for each lens that is compliant enough to attenuate irregularities of the mounting surface.
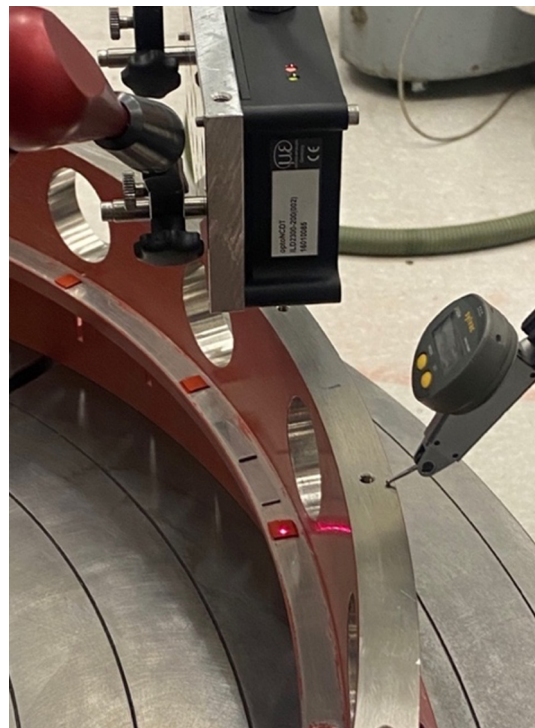

Fig. 10 Image of the L1 axial pads being measured using the laser displacement sensor. Measurements were taken in the center of the pad as can be seen from bright spot on the pad where the laser beam hits. Figure also shows the angled surface where the axial pads rest along with the radial insert holes.
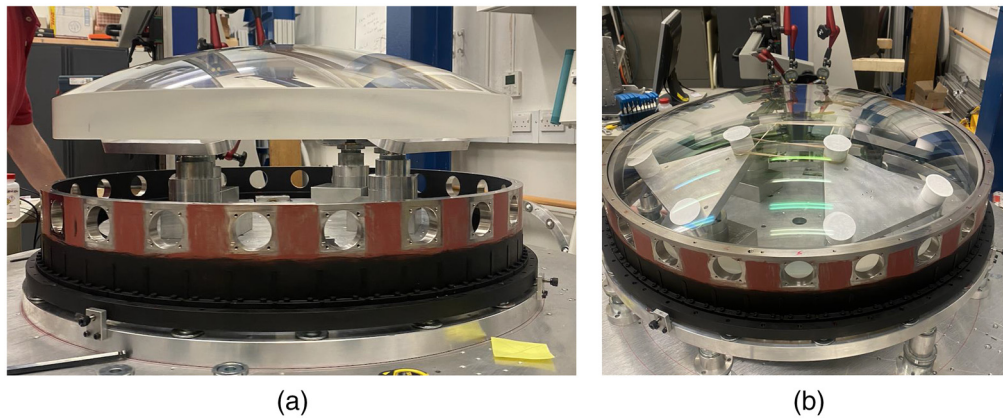
Fig. 11 (a) L1 lens being supported on the whiffletree structure on the rotary table before being put into its cell. (b) L1 lens resting on the axial pads in L1 cell before the RTV pads are inserted (the white visible circles shown are where the whiffetree structure is supporting the lens).

4.2 Lenses into Cells

The cell design for L1 and L4 used are very similar to that used in other work[7] and consisted of an angled surface where the axial pads would be glued to and where the lens would rest, along with periodic holes on the sides of the cell where the radial pads would be inserted to hold the lens in position (see Figs. 10 and 11) To insert a lens into its cell, the lens is placed on a distributive load support system (whiffletree-like stage, shown in Fig. 11). Extreme care was taken to space the support points of the whiffletree system so that the lens did not distort in anyway. More details of a similar process can be found in the literature for similar WFC projects, such as DECam on the Blanco Telescope.[7,9]

Placing the lenses in their cells is a complicated and slow process. Raising the cell to the supported lens ensuring the cell was kept level at all sides by slowly raising each jack to the correct height until the axial pads within the cell meet the lens. The larger jacks move the lens cell into place by carrying out larger movements ($\sim$100 μm). Once the lens cell was close enough to the lens (within 2mm), the jacks were replaced with aluminium posts and precision screw jacks to raise the lens cell in finer incremental steps ($5 - 10$ μm). A dial gauge was used to ensure all sides were raised equally until the pads began to make contact with the lens. At this stage, the positions of both the lens and the cell were measured again to establish their positions before the radial pads were glued in place.

To attach the radial pads the following procedure was used. The radial pads on their inserts were first were screwed in but not glued to the lens but instead had a paper of a suitable thickness
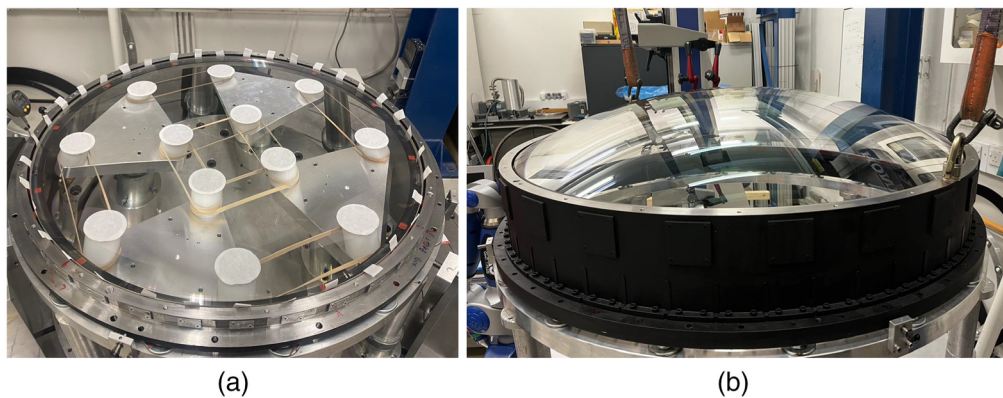

Fig. 12 (a) L4 lens in its cell with the 40-μm paper stopping the RTV pad inserts from touching the lens before they get glued in place. (b) Final assembly of L1 lens in L1 cell after RTV pads have been inserted and rest of the L1 cell has been painted black.
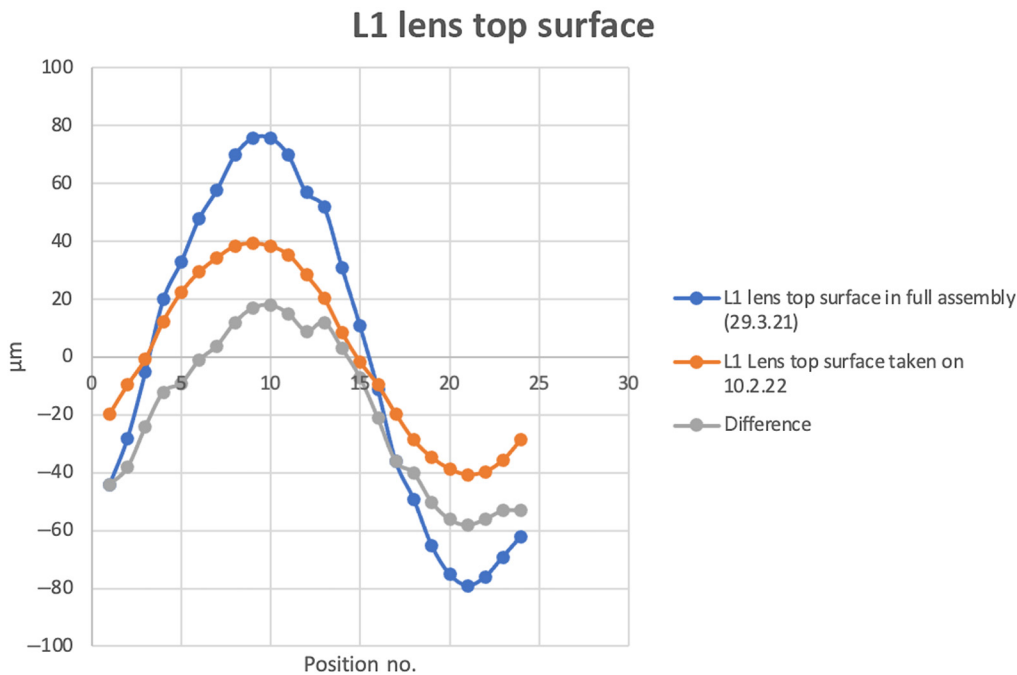
L1 lens top surface

Fig. 13 Example showing the L1 lens top surface variation comparing flatness before and after being put into full assembly, along with the difference between them. Measurements taken using a dial gauge, showing the assembled L1 lens top surface to be within ±80 μm.

(~40 μm) to take up the gap between the RTV of the radial pads and the lens outer diameter (see Fig. 12). This locked the entire system in position. Opposite pairs of the radial pads were removed and the glass was primed before the freshly glued RTV pads were reinserted. Two pairs of opposing pads at 90 deg to each other were glued in at a time and allowed to cure, this was continued until all pads were inserted to ensure minimal movement in any one direction of the lens until the process was complete and the lens was fully glued to the cell. The same procedure was carried out for both L1 and L4.

All lenses were put into their cells to minimise the bottom surface run out (bottom surface refers to the surface closest to the FSP), so that a wedge (if any) would be expressed on the top surface. The L1 lens was deliberately offset in the cell by ~70 μm in X and ~30 μm in Y to ensure the L1 asphere was centered such that the top surface run out was zeroed. This left a wedge expressed on the upper surface with a run out of ±40 μm on the top surface (well within the wedge tolerance). When put into the full final assembly, this changed to ±80 μm (Fig. 13). This additional run out expressed when in final assembly could also be explained by both the variation in the flatness of the surfaces when mated and also a projection effect, as L1 is sitting on-top of the tall barrel, if there were a few microns tilt at the bottom, this could express an increased run out on the top. This increased run out is due either to lens decenter or a tilt of the lens—but is well within tolerance.

5 Laser Alignment Test

5.1 *Setup*

As an additional check to the contact metrology measurements for the alignment of the lenses, an LAS[7] was built at UCL to test the relationship between L1 and L4 in the assembled system without the ADC optics (see Figs. 14 and 15). The WFC was assembled in two variations on the rotary table to cater for the tests to be carried out on L1 and L4 (one system with L1 and L4 together, and another system with just L4). Prior to the lenses being put in, tests were carried out using a retro-reflector and a corner-cube to check the parallelism and centring of the laser on the rotary table. Once the system to be tested was set up and aligned with the L1 and L4 lenses in
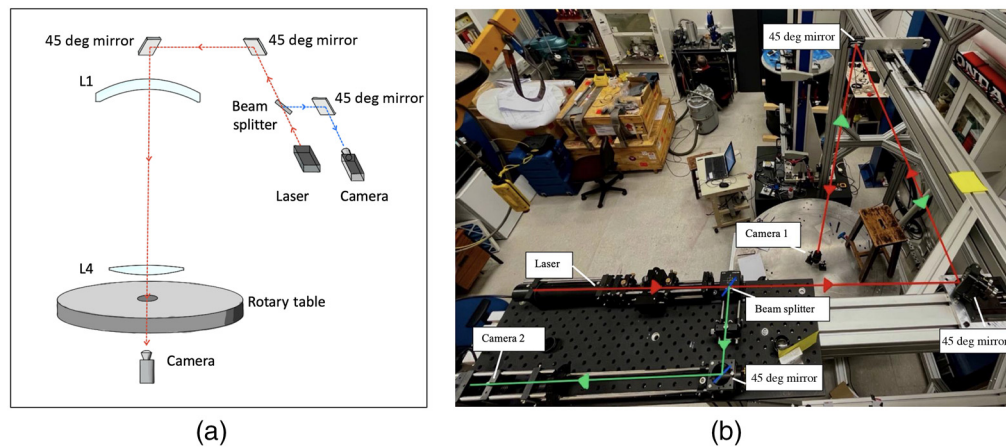
Fig. 14 (a) Labeled schematic of the LAS used to test the optics. The red arrow indicates the path the laser beam takes, hitting a two 45° deg mirrors before passing through the WFC system, the rotary table and through to the camera for the through beam. The blue arrows indicate the reflected path of the laser beam going into the second camera. (b) Showing a photo of the LAS set up in the lab.

position, it was then rotated through 360 deg taking measurements at every 90 deg. Two cameras were installed, one below the rotary table to capture the through beam of the laser and one above, to capture the reflected beam. This test was carried out to test four key elements; the through beam of L4, the reflected beam of L4, the through beam of L1 and L4 together and finally the reflected beam of L1. The main aim of these tests was to check that L1 and L4 were aligned to within the measured uncertainties, that L1 was consistent with L4 when assembled in the barrel and that the results coordinated with the contact metrology measurements. Both the L1 and L4 centroids found with the LAS system confirmed that our centers and tilts were well within the required tolerances for both L1 and L4 (see Table 2).

6 Alignment Results and Final Assembly

The assembly requirements were dictated by the lens alignment and lens tolerances (can be found in Table 1). After all lenses were potted in their cells and all measurements of the components taken, including distances from each lens to the focal surface (this was done to check what shim thicknesses were needed to ensure correct distances for the focal length of each lens), the first step in final assembly was aligning the L2/L3 lenses to the L3 OBP and integrating it into the ADC unit. The L3 OBP was our main reference surface as this was one of the few surfaces we could reach for the majority of the measurements. L4 and tube D were subsequently integrated to the ADC and together the whole ADC unit including L4 and tube D were bolted to the MSP [Fig. 19(b) and 19(c)]. This initial assembly of the lower section of the WFC was carried out on the rotary table and supported using jacks. After the lower section had been integrated to the MSP, the outward facing surface of L2 was blackened using a Edding 800 permanent black marker to ensure no other stray light missed by the internal baffles could reach L3/L4. The system was then moved off the rotary table and onto the WFC trolley for the rest of the assembly due to height restrictions of the crane, which was used to move the elements. Tube A, along with its baffles was added to the MSP before finally the L1 lens and cell were added (baffles are used to prevent excess scattering of light within the system that may adversely effect the incoming light). Tests were carried out at each stage of the final assembly to ensure everything was consistent with our previous measurements. "Loctite 243" was applied to the bolts before insertion to ensure bolts were secure and to prevent loosening. Images of final assembly process can be found in the Appendix.

6.1 *Off-Axis Laser Pencil Beam*

After final assembly was complete, a laser pencil beam (LPB) tool was used to test the optics of the WFC for pre and post delivery to Leibniz Institute for Astrophysics, Potsdam (AIP).
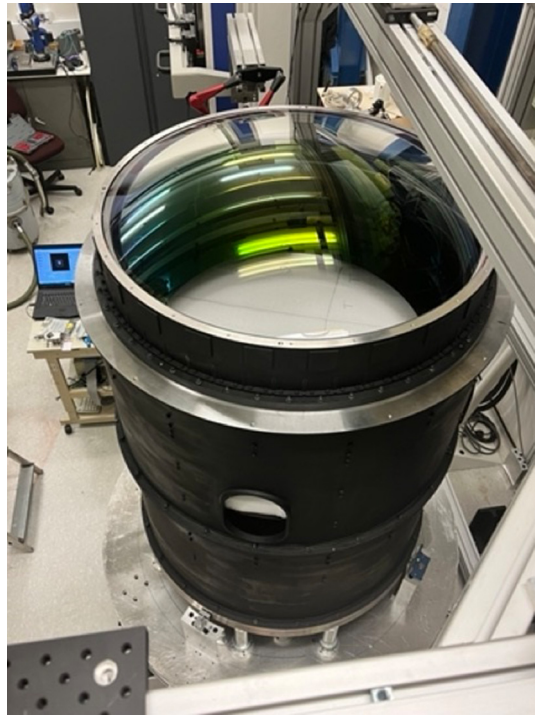
Fig. 15 Top-down view of the WFC assembly on the rotary table (without L2 and L3 inserted). L1 lens is shown at the top and is where the laser enters first. Just below L1 there is polystyrene foam that was added to stop any reflections from the L4 lens interfering with the L1 reflected beam. This was also used to stop things falling onto the L4 lens.

The laser was set up as shown in Fig. 16. An off-axis laser beam was sent through the system and the reflection of each lens surface was captured by a built-in camera which recorded the reflected image position. On arrival to AIP, the same test was carried out to verify and check if there was any movement of the optics during transportation. If the lenses had moved, this would be revealed during the LPB test, however the WFC was successfully delivered and all lenses were found to be within the measurement tolerances.
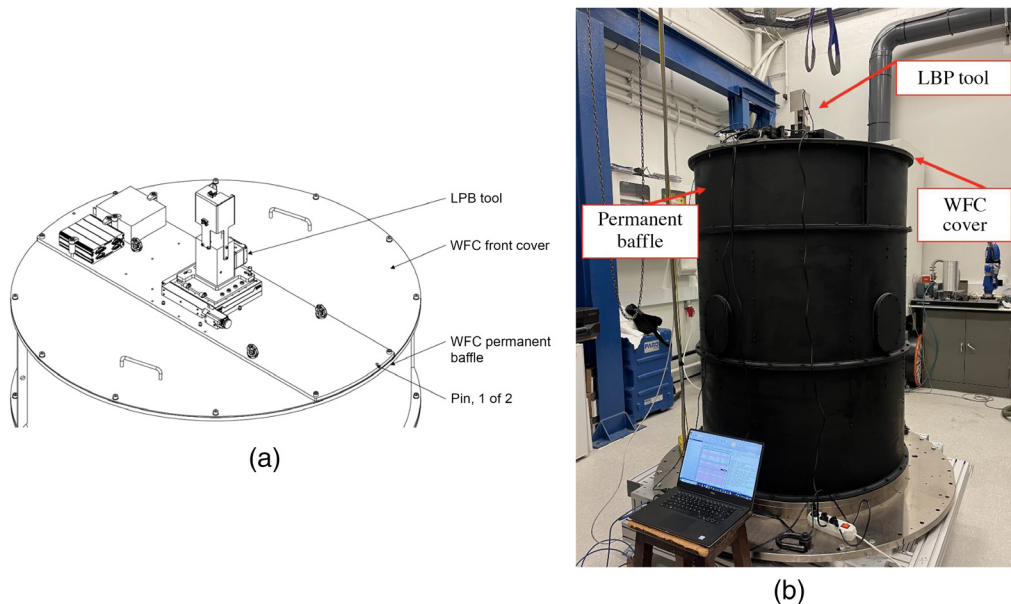

Fig. 16 (a) Schematic of the LPB Tool that was used to test the movement of the lenses pre- and post-delivery to AIP. (b) Image of the LPB tool during testing.

Table 2 4MOST lens alignment results.

Lens	Lens decenter (X, Y) (μm)	Tolerance (X, Y) (μm)
L1	(−41.75, 15.13)	200
L2	(19.51, −16.04)	1000
L3	(6.79, 7.10)	100
L4	(22.27, −7.65)	200

6.2 Lens Centers

The final lens center positions for each lens in the final set up are shown in the table below and as shown in Fig. 17. All lenses were compared to the L3 OBP as this was our reference center. All lenses fall within the decentering tolerances given for each lens.

6.3 Lens Tilts

As previously described each lens's bottom surface run out was minimised when put into its cell, this left any lens wedge and any residual tilt to be expressed on the top surface measured as a run out. When the lenses were installed into the full assembly the top surface run out was remeasured. Table 3 describes the initial lens surface variations in the cell pre-assembly after the lenses have been mated into their cells and the lens surface variations after the lenses have been put into the
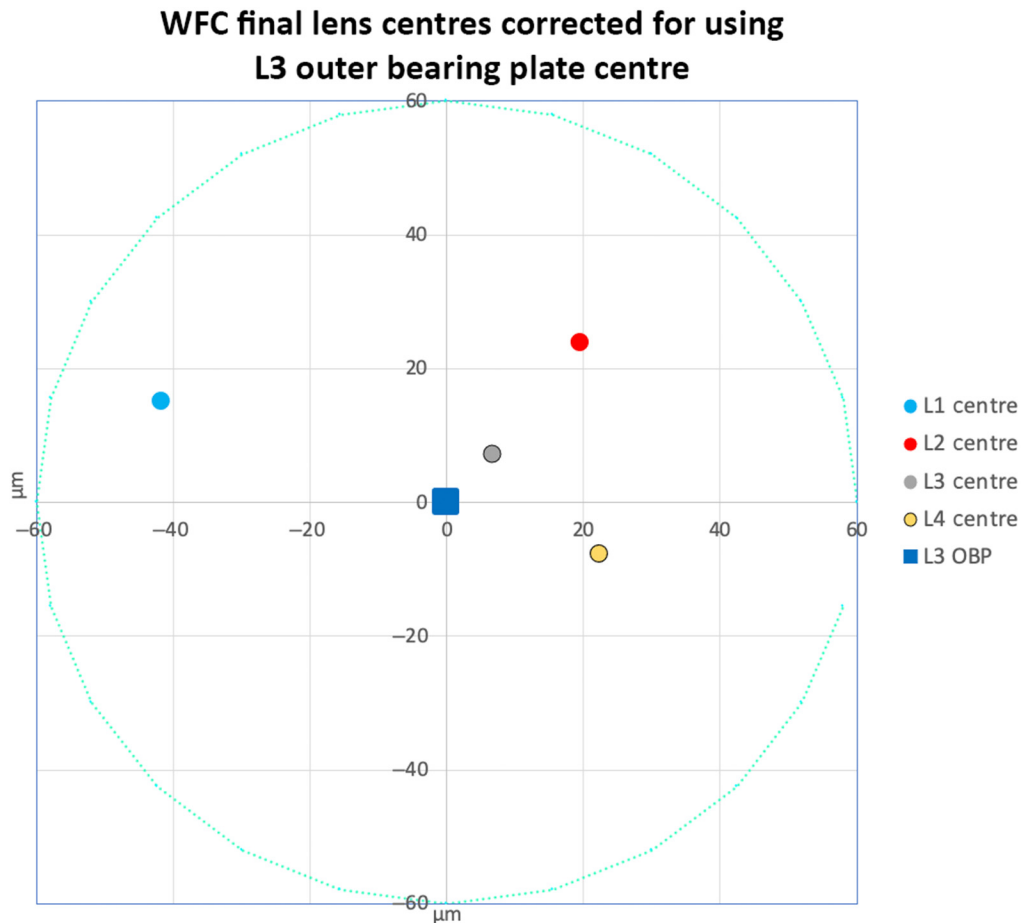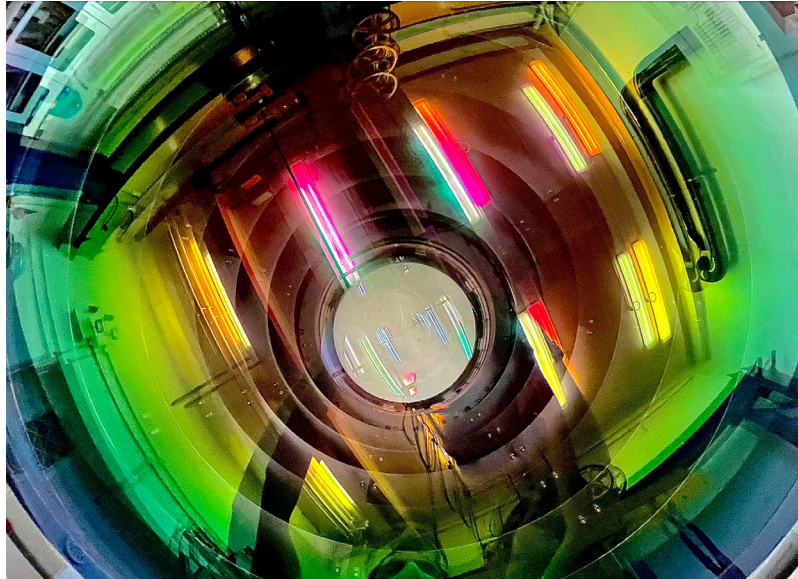

Fig. 17 Plot showing the WFC lens centers after installation in barrel relative to the target center of the L3 OBP.

Table 3 The WFC Lens tilts calculated from the lens surface run outs.

Lens	Initial lens surface variation (μm)	Lens surface in full assembly (μm)	Change in variation (μm)	Tilt angle (μrad)	Tilt tolerance ($\pm\mu$rad)
L1	80	155	75	83.33	785
L2	489	647	78.46	83.33	945
L3	8	47	75	60	95
L4	67	68	19	29.23	142

Fig. 18 A look through the full WFC system looking directly down the L1 lens. The inner baffles are shown along with the dispersion of the laboratory lights.

full WFC assembly. The difference between the two variations was calculated (this accounted for positional variation also) and the tilt angle found. All lens tilts lay well within the given tolerances.

7 Conclusion

All lenses were successfully installed into the corrector, without damage and well within the allotted tolerance. The corrector was successfully shipped to AIP with no movement of the optics during transportation and will begin integration with the AESOP fiber positioning unit before continuing its journey to the telescope. Further tests will be carried out on the WFC while at AIP, such as transmission tests. This transmission test will shoot different light sources (IR to UV) in varying positions through the WFC, and measure throughput with a photo diode sensor. When the WFC eventually makes its way to Chile, further integration and tests will need to be carried out on site to test the optical image of the WFC to ensure the instrument has not moved again during shipment and to guarantee that the WFC meets its scientific goals.

8 Appendix A: Assembly Process

Figure 19 shows the process that took place during the final assembly of the WFC in the laboratory at UCL. It should be noted that during each stage of integration during the final assembly, measurements were taken to ensure our alignment had not changed.

A table of the metrology instruments used during assembly and alignment can be found in Table 4 along with their respective accuracies.
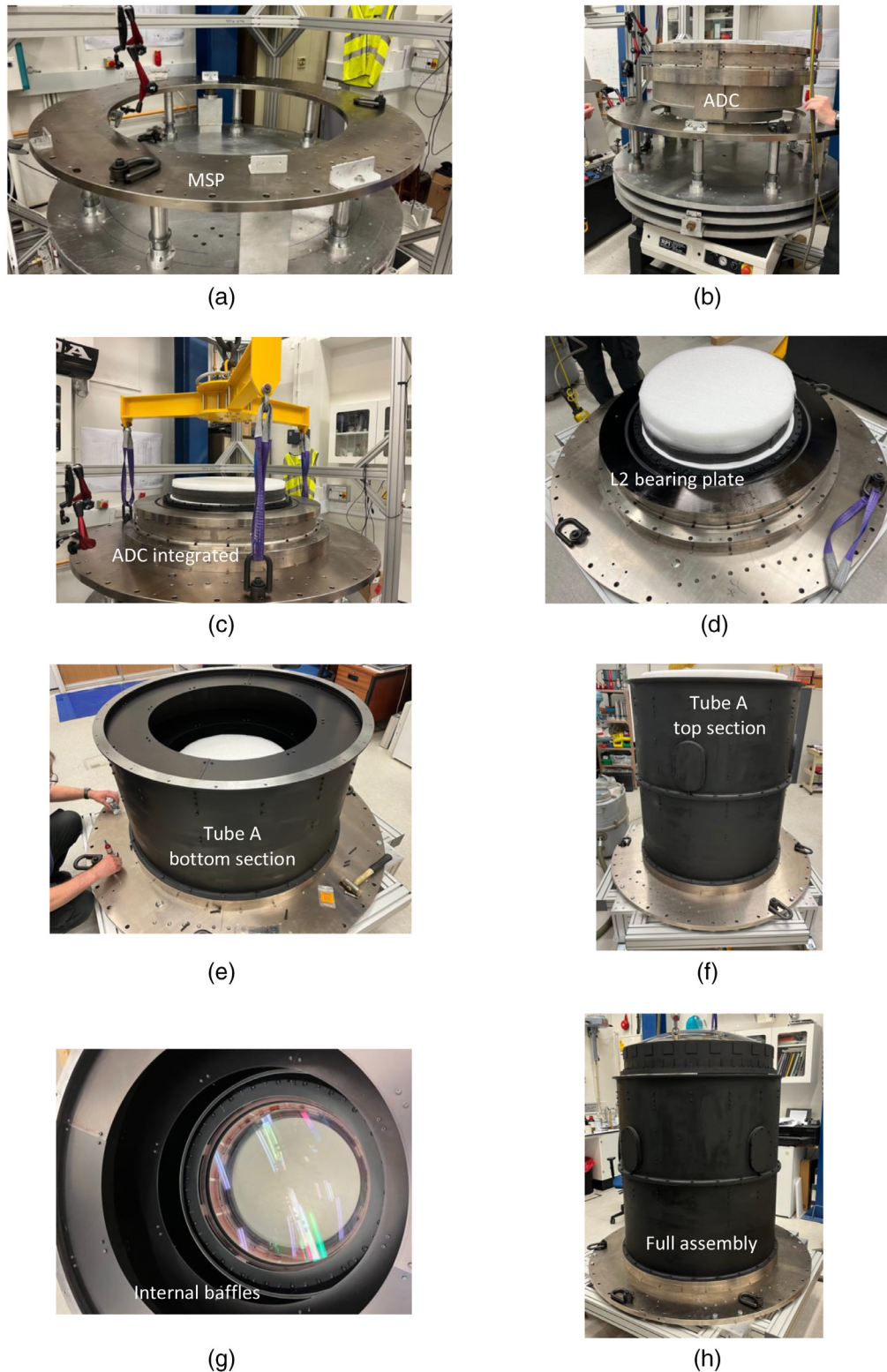
Fig. 19 Final assembly of the WFC after all lenses have been aligned to the system. Measurements were taken at each stage to ensure alignment had not changed. (a) MSP and (b) ADC being lowered into the MSP. (c) ADC unit integrated with MSP. (d) L2 bearing plate with blackened surface in ADC unit. (e) Tube A part (ii) integrated with MSP and ADC. (f) Tube A fully integrated. (g) Look down at the internal baffles of tube A. (h) Fully assembled WFC with L1 integrated.

Table 4 Table showing the accuracy of the metrology instruments used throughput the assembly and integration of the WFC.

Metrology tool	Accuracy of instrument (μm)
Micrometre	± 5
Dial gauge	± 2
Faro gage arm	± 10

Acknowledgments

References

1. R. Ellis et al., *The Future of Multi-Object Spectroscopy: A ESO Working Group Report* (2017).
2. R. S. de Jong et al., "4MOST: the 4-metre multi-object spectroscopic telescope project at preliminary design review," *Proc. SPIE* **9908**, 99081O (2016).
3. R. S. de Jong et al., "4MOST: 4-metre multi-object spectroscopic telescope," *Proc. SPIE* **8446**, 84460T (2012).
4. J. Brzeski et al., "AESOP: the 4MOST fiber positioner," *Proc. SPIE* **10702**, 1070279 (2018).
5. N. Azais et al., "Wide field corrector for 4most: design details and maiv processes," *Proc. SPIE* **9908**, 990889 (2016).
6. M. Antonik et al., "The design and alignment of the DECam lenses and modelling of the static shear pattern and its impact on weak lensing measurements," *Proc. SPIE* **7433**, 74330M (2009).
7. P. Doel et al., "Assembly, alignment, and testing of the DECam wide field corrector optics," *Proc. SPIE* **8446**, 84466F (2012).
8. R. G. Fata, V. Kradinov, and D. Fabricant, "Mounting large lenses for the MMT's f/5 wide-field corrector: lessons learned," *Proc. SPIE* **5492**, 553–563 (2004).
9. K. Honscheid and D. L. DePoy, "The dark energy camera (DECAM) a new instrument for the dark energy survey," in *2008 IEEE Nuclear Sci. Symp. Conf. Record*, IEEE (2008).
10. M. Cunningham et al., "The assembly and alignment of the 4MOST wide field corrector," *Proc. SPIE* **12184**, 121846V (2022).

Mark H. Cunningham is a current PhD student at University College London (UCL). His research is a unique hybrid between astronomical instrumentation and high redshift galaxy spectroscopic data analysis. The principal aim of his research project has been to align, assemble, and integrate the wide-field corrector for "4MOST," the 4-metre multi-object spectrograph telescope. The secondary aim of his research focuses on the analysis of emission lines in high redshift galaxies to try and uncover the mystery of the Epoch of Reionisation; one of the last eras in the Universe to be fully understood.

Peter Doel graduated from Durham University in 1986. His PhD was at Durham in the astronomical instrumentation group, where he was involved in adaptive optics (AO) systems. He joined UCL as a lecturer in 1998, and his research since then has included development of coronographic systems, carbon fiber mirrors, and wide field survey optics, including the optical correctors for the dark energy survey camera, the dark energy spectroscopic instrument, and the 4MOST multi-object spectrometer.

David Brooks is working as a professorial research fellow, Optical Science Laboratory, Department of Physics and Astronomy, University College London. He was awarded his PhD in 2001 and has been an expert in optics and optical instrumentation for over 38 years. He produced 1.83-m-diameter 1.4 tonne aluminium primary mirror for the Birr Telescope along with an assortment of spectrographs, cameras, and three optical correctors for dark energy surveys.

Joar Brynnel has been active in the field of telescopes and instrumentation for astronomy since 1990. At ESO (Garching, Germany), he participated in several instrument and adaptive optics projects for the La Silla and Paranal observatories. Between 1998 and 1999, he was stationed on the Paranal observatory during the first year of VLT science operations. From 2003 until 2014, he was employed by the University of Arizona, working at the LBT observatory as engineering group manager and commissioning manager. In 2014, he was appointed project manager for the 4MOST project at the Leibniz Institute for Astrophysik in Potsdam, Germany, where he also heads the project management department.

Roelof S. de Jong is working as a head of the Milky Way and the Local Volume section at the Leibniz Institute for Astrophysics Potsdam (AIP). His main research area is studying the formation and evolution of nearby disk galaxies, including the Milky Way. He is furthermore the principal investigator of the 4-metre multi-object spectroscopic telescope (4MOST) project, bringing a fiber-fed, wide-field and high-multiplex optical spectroscopic survey facility to ESO's 4-metre class VISTA telescope.

Steffen Frey is working as an systems engineer at the Leibniz Institute for Astrophysics Potsdam (AIP). He is also the work package manager for 4MOST on system integration, installation, and maintenance.

Michael Schroeck is working as a mechanical engineer at Leibniz-Institut für Astrophysik Potsdam (AIP), responsible for manufacturing, assembly, and test/integration of the WFC at AIP. Previously, he was a mechanical engineer at Roschiwal + Partner GmbH working on project-oriented work for, i.e., the automation of battery production or the development of an autonomic deconstruction saw for nuclear reactors. Prior to this, he worked at Aluminium Werk Berlin GmbH (AWB), where he was a quality assurance engineer, which also included quality management activities.

Miklos Gaebler with deep technical expertise in aerospace propulsion systems and two decades of industrial experience in complex system technology development and validation, provides his knowledge and personal guidance to the 4MOST project challenges to minimize the risks and meet the project timelines of the WFC subsystem covered under WP.6.2

Daniel Sablowski received his PhD at the University of Potsdam and the AIP on the topic of stellar spectral analysis and spectral disentangling. Currently, he is working as an instrumentation scientist at the Leibniz Institute for Astrophysics Potsdam (AIP) in Germany. He is specialized in spectroscopic instrumentation with a focus on high spectral resolution (echelle) spectrographs. Currently, he is working on the ESO 4MOST instrument on several subsystems from the wide-field corrector over acquisition and guiding to system integration and verification.

Sam C. Barden is working as a system's engineer at the Maunakea Spectroscopic Explorer. Prior to this, he was working as a work package manager for the 4MOST wide field corrector and other subsystem components. He has an extensive background in astronomical spectrographs, fiber optics, as well as optical design.